Arktos (2015) 1:8
DOI 10.1007/s41063-015-0010-z

ORIGINAL ARTICLE

Variable influx of West Greenland Current water into the Labrador Current through the last 7200 years: a multiproxy record from Trinity Bay (NE Newfoundland)

C. M. Sheldon[1] · M.-S. Seidenkrantz[1] · P. Frandsen[1] · H. V. Jacobsen[1] · N. Van Nieuwenhove[1] · S. Solignac[1,2] · C. Pearce[1,3] · M. G. Palitzsch[1] · A. Kuijpers[4]

Received: 2 September 2015 / Accepted: 13 October 2015 / Published online: 20 November 2015

Abstract A multiproxy study of marine sediment gravity core AI07-06G from Trinity Bay, Newfoundland, recorded changes in the strength of the Labrador Current (LC) during the Holocene. From ca. 7.2–5.7 cal kyr BP, Trinity Bay's seafloor was influenced by cooled Atlantic water derived from the West Greenland Current (WGC) Davis Strait branch, merging into the relatively cold LC. This Atlantic water influence gradually decreased after ca. 5.7 cal kyr BP, reaching a minimum at ca. 4.9 cal kyr BP. In contrast, surface temperatures were relatively low due to cold surface water dominated by sea ice and meltwater carried south by the LC. Icebergs from outlet glaciers around Baffin Bay were abundant in the LC prior to ca. 5.5 cal kyr BP. From ca. 4.9–2.9 cal kyr BP, bottom waters became slightly colder and salinity decreased, as increased mixing of the water column brought less saline surface waters towards the seafloor. This may be explained by a weaker North Atlantic subpolar gyre, transporting less Atlantic water from the WGC to the (outer) LC. Arctic meltwater transport was reduced as glacial melting decreased at the end of the Holocene Thermal Optimum. At ca. 2.9 cal kyr BP, bottom waters returned to colder, more stable conditions, indicating a slight decrease in bottom-water ventilation. After ca. 2.1 cal kyr BP, surface water temperatures dropped and sea ice flux increased. The seafloor of Trinity Bay saw warmer conditions, consistent with a stronger subpolar gyre and increased influx of Atlantic-sourced water.

Keywords Holocene · Labrador Current · Gulf Stream · North Atlantic subpolar gyre · Arctic meltwater

Introduction

The Labrador Current (LC; Fig. 1a) is an important component of the modern North Atlantic circulation, including the formation of deep and intermediate water masses in the North Atlantic subpolar gyre [85, 123], an integral part of the global thermohaline circulation system [45, 85, 100]. The LC helps to export the buoyant, fresher water from the Arctic Ocean and Baffin Bay to the North Atlantic, where it forms the western boundary of the North Atlantic subpolar gyre [84]. In contrast to the inner (nearshore) component of the LC, which is almost solely made out of cold Polar Water from the north, the outer (offshore) component also transports warmer, Atlantic-influenced water from the West Greenland Current, although the strength of this Atlantic water transport, as well as its variability, is still unclear.

The relative strengths of the main currents in the subpolar gyre (Fig. 1a) have been intimately tied to abrupt climate changes in the past [15, 16, 47, 119], due to the gyre's role as a site of intermediate- to deep-water formation [14, 72, 94, 101]. The importance of the LC in

Electronic supplementary material The online version of this article (doi:10.1007/s41063-015-0010-z) contains supplementary material, which is available to authorized users.

✉ C. M. Sheldon
christina.sheldon@geo.au.dk

[1] Department of Geoscience, Centre for Past Climate Studies and Arctic Research Centre, Aarhus University, Høegh-Guldbergs Gade 2, 8000 Aarhus, Denmark

[2] GEOTOP, Université du Québec à Montréal, P.O. Box 8888, Montréal, QC H3C 3P8, Canada

[3] Department of Geological Sciences and Bolin Centre for Climate Research, Stockholm University, Svante Arrhenius väg 8, 106 91 Stockholm, Sweden

[4] Geological Survey of Denmark and Greenland (GEUS), Øster Voldgade 10, 1350 Copenhagen K, Denmark

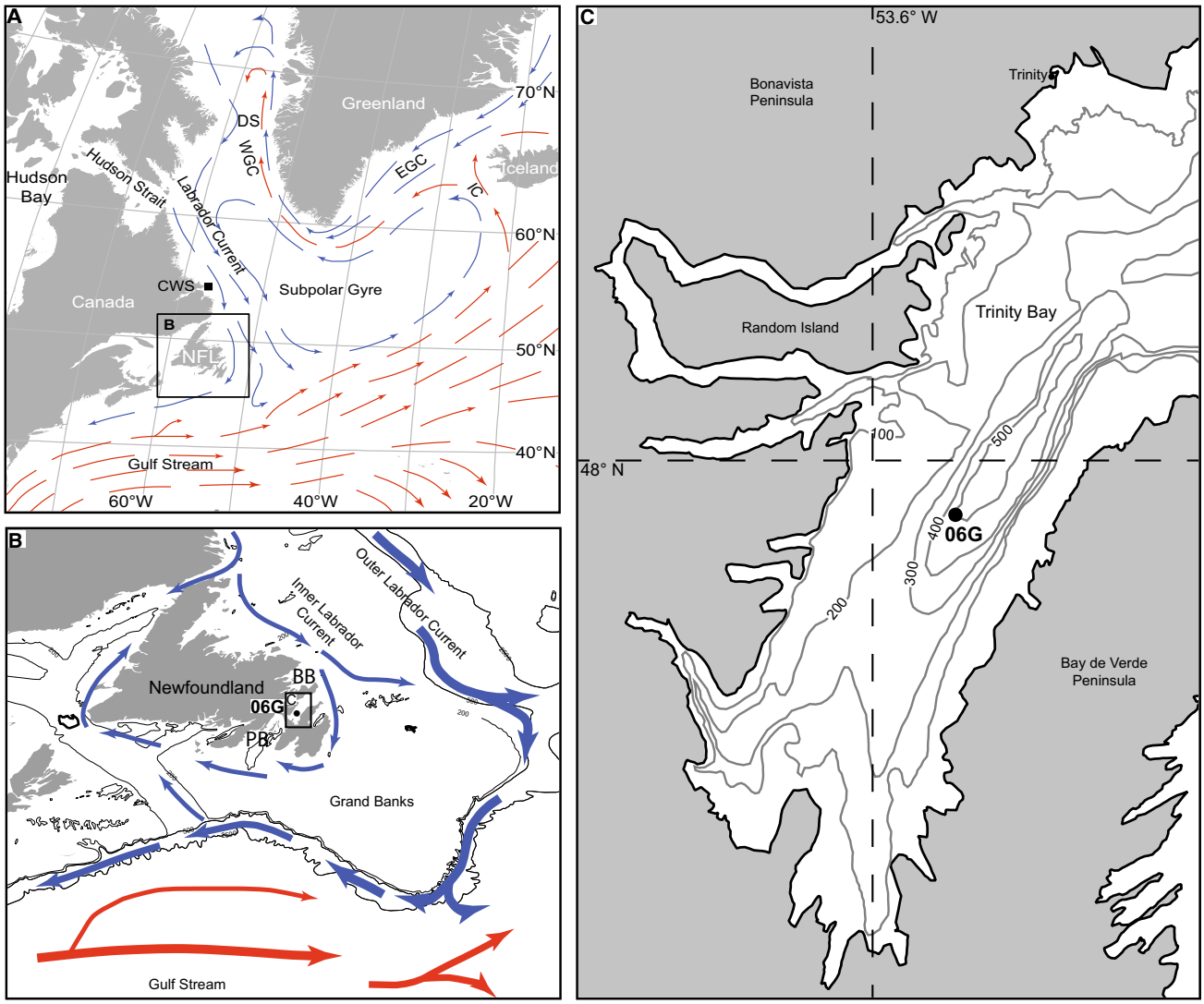

Fig. 1 Map of study area, including major currents impacting both the study site and the subpolar gyre. *Red arrows* 'warm' currents, *blue arrows* 'cold' currents. **a** Modern oceanographic conditions of the Labrador Sea region. The Labrador Sea is bounded by the West Greenland Current (WGC) to the east and by the Labrador Current (LC) [19, 56, 115]). The WGC is comprised of cold, Arctic-sourced East Greenland Current (EGC) water and warmer, Atlantic-sourced Irminger Current (IC) water. *WGC* West Greenland Current, *EGC* East Greenland Current, *IC* Irminger Current, *DS* Davis Strait, *NFL* Newfoundland, *CWS* Cartwright Saddle. The *square* shows the area given in detail in **b**. **b** Detailed map of the Newfoundland region; *BB* Bonavista Bay, *PB* Placentia Bay. The *square* shows the area given in detail in **c**. 06G = gravity core AI07-06G. **c** Detailed map of the bathymetry of Trinity Bay based on information from nautical charts. Dot = location of core AI07-06G (06G)

North Atlantic Ocean circulation makes refining its development, especially after the last glacial period, useful in reconstructions of past climate and oceanography [38, 106, 110]. Both the density- and wind-driven components are important for the nearshore (inner) part of the LC. In contrast, the density-driven component dominates the mean shelf edge (outer) LC, with wind forcing of primary importance for its seasonal variability [44].

The region of Newfoundland is located at the oceanic frontal zone between the LC and the Gulf Stream (GS) (Fig. 1a, b). This makes this region ideal for studying the frontal movements between the LC and the GS, as well as the strength of the Atlantic water influence in the LC. Trinity Bay, on the north-eastern seaboard of Newfoundland (Fig. 1b, c), lies just north of the core of the frontal zone and thus carries a strong LC signal [122]. Since 1950, regular hydrographic observations have been made on the nearby 'Bonavista transect' extending from the coast of Bonavista Bay to the Northern Grand Bank [17]. These measurements show the presence of a large volume of below 0 °C subsurface water mass during summer and autumn ('cold intermediate layer'), situated between a mixed surface layer and

the deeper, warmer LC slope water (derived from the outer LC) near the bottom over the outer shelf [73]. Based on these modern observations, there is no indication of penetration of GS water onto the shelf this far north.

The modern hydrography of Trinity Bay and its link to the wind system have been investigated by Yao [122], but previous investigations on variability in regional climate and ocean circulation on a geological timescale have focused on nearby bays in Newfoundland. These studies found that the Labrador Sea has been strongly affected by the Labrador Current (LC), transporting meltwater from the Arctic and Hudson Strait region through the Pre- and Early Holocene. The Cartwright Saddle, north-east of Newfoundland, recorded several glacial outburst events from Hudson Strait in the late glacial and Early Holocene periods [51]. After major oceanographic shifts in the Younger Dryas (YD) and the Early Holocene [77, 78, 109], the oceanographic regime of the Labrador Sea underwent reorganisation several times [38, 48, 77, 90, 107, 109], also prior to the generally more unstable period of the last ca. 3000 years [95, 106, 108, 110]. Large quantities of glacial meltwater caused harsh sea surface conditions in the southern Labrador Sea in the Mid- to Late Holocene, both north and south of Newfoundland [112]. Atmospheric and ocean circulation changed in response to changes in the mode of the North Atlantic Oscillation/Northern Annular Mode during the Late Holocene [55], which may also explain an increase in sea ice recorded over the past 150 years in the southern Labrador Sea [121].

None of the studies so far have investigated the Atlantic water component carried by the (primarily outer) LC or its potential influence on nearshore regions, despite the significance of Atlantic-sourced water in subpolar gyre heat and salt transport and deep convection. The present study thus intends to reconstruct the varying strength of the Labrador Current and the potential influence of Atlantic-sourced water in the LC, impacting the subpolar North Atlantic Ocean circulation, during the Mid- to Late Holocene. Through the reconstruction of the Labrador Current strength and variation in the LC Atlantic water component, changes in ocean circulation in the North Atlantic are evaluated.

Modern environmental setting

Trinity Bay is a large embayment located on the north-east coast of Newfoundland, at the south-western margin of the Labrador Sea (Fig. 1a). The bay is 100 km long by 30 km wide, with a maximum water depth of 590 m, a sill depth of 240 m [76, 122] and variable bottom topography (Fig. 1c). In summer, a pycnocline is formed at approximately 25 m water depth, with fresher surface waters capping the comparatively more saline waters filling most of the bay [122]. Trinity Bay receives run-off from local rivers on north-eastern Newfoundland, although this contribution is relatively small. Monthly sea surface temperatures in Trinity Bay vary between −0.5 in March and 13.0 °C in August [66], and monthly salinity in August ranges from 30 to 31 [122] and in May from 32.5 to 33 [103].

Today, Trinity Bay is flushed by the southward-flowing inner Labrador Current (LC), which is formed by cold, relatively low-salinity water entering Baffin Bay through the Canadian Arctic Islands and Nares Strait [19] (Fig. 1a). In Baffin Bay and the northern Labrador Sea, the LC mixes to some extent with water from the WGC, via the North Atlantic subpolar gyre (Fig. 1a). Entrained in the WGC is warm, saline water from the Irminger Sea, carried by the Irminger Current [19], and cold, low-salinity water from the Arctic Ocean relayed by the East Greenland Current. Today, the Atlantic-sourced component is primarily found in the outer (offshore) LC, while the inner (nearshore) LC is, to a larger extent, characterised by Arctic water and freshwater outflow from Hudson Strait [70]. The modern oceanic front between the LC and the Gulf Stream (GS) is located south of Trinity Bay. Thus, while the southern coast of Newfoundland is characterised by influx of both LC and GS water today [29, 70] as well as in the past (e.g. [77, 78, 109, 110]), the oceanographic conditions at the north-eastern margin of Newfoundland, including Trinity Bay, are today dominantly influenced by the LC [70]. Consequently, changes in the strength or heat transport of the GS do not directly influence the northern coast of Newfoundland, as the Atlantic water component that reaches Trinity Bay is first transported by the Irminger Current, the West Greenland Current, and finally around the northern sector of the subpolar gyre before mixing with the cold LC. Thus, any change in Atlantic water influence in Trinity Bay is primarily linked to the strength and position of the subpolar gyre, although that is, of course, again influenced by the strength of the GS and its derivatives.

Newfoundland lies in the path of westerly winds and is impacted by air masses from both the north and the south. Winds are strongest in winter, with westerly to north-westerly winds bringing Arctic air to Newfoundland (Trinity Bay region) [7]. In contrast, the southern coast receives warm, moist air from the Gulf Stream [12]. In summer, winds are weaker and of south-west origin over the entire island [7]. These winds influence the impact of the LC and GS on Newfoundland. Nevertheless, the impact of the GS is generally stronger in the south, and the LC is generally stronger in the north; this leads to a clear north–south air temperature gradient. Periods of positive North Atlantic Oscillation increase northerly winds and decrease temperatures in the region [29, 81, 83].

Table 1 Radiocarbon materials and associated dates from core AI07-06G, used to create the age model for the core

Laboratory number	Depth (cm)	Material	^{14}C age ± 1σ	Calibrated age range 95 % confidence (cal BP)		Modelled mean age (cal year BP)	δ^{13}C ‰
AAR-16847	3–8	*N. labradorica* (foraminifera)	668 ± 25	271	Modern	151 ± 79	−3.06 ± 0.05
AAR-16848	44–45	Mixed foraminifera	1078 ± 25	648	452	547 ± 52	−1.92 ± 0.05
AAR-16849	74–76	Mixed foraminifera	1513 ± 25	1066	756	918 ± 78	−2.00 ± 0.05
AAR-16850	93–95	Mixed foraminifera	1617 ± 25	1185	895	1034 ± 76	−1.46 ± 0.05
AAR-16851	154–156	Mixed foraminifera	2448 ± 25	2105	1765	1927 ± 84	−1.77 ± 0.05
AAR-16852	244–246	Mixed foraminifera	3431 ± 26	3319	2943	3124 ± 97	−1.84 ± 0.05
AAR-16853	354–356	Mixed foraminifera	486 ± 27	5230	4835	5017 ± 108	−1.19 ± 0.05
AAR-16854	413–415	Mixed foraminifera	6331 ± 35	6801	6445	6629 ± 89	−0.74 ± 0.05
AAR-12116	428–431	Mixed foraminifera	6776 ± 49	7325	6954	7152 ± 93	−0.98 ± 0.05

In the central Labrador Sea sector of the subpolar gyre, the combined effect of the cold northerly winds and the influx of saline waters leads to deep to intermediate water formation known as Labrador Sea Water (LSW; [123]). The varying influxes of saline, Atlantic-sourced water, and fresher water from the Arctic lead to variations in the strength of LSW formation in the subpolar gyre [8], influencing the Atlantic Meridional Overturning Circulation (AMOC) [45, 115].

In addition, the LC is responsible for a significant portion of the freshwater export from the Arctic. It transports icebergs originating from (north)western Greenland and from the Canadian Arctic Islands southward out of Baffin Bay through Davis Strait [4, 97, 112]. Sea ice found off the north coast of Newfoundland is mostly advected from Baffin Bay [29] and enhanced when north-westerly winds are strong [22, 29, 81, 83]. However, some sea ice affecting northern Newfoundland can form locally in the Labrador Sea [22, 83], as well as in northern Newfoundland bays [27]. However, little sea ice forms in modern Trinity Bay [10].

Materials and methods

The 431-cm-long gravity core AI07-06G (hereafter 06G; 47.85N, 53.58W) was taken from Trinity Bay, north-eastern Newfoundland, during a 2007 cruise aboard the Russian research vessel *Akademik Ioffe*. The water depth at the core site was 511 m. The core was split in half lengthwise in the laboratory, and both halves were placed in cold storage at 2 °C. The 'archive half' was used for X-ray fluorescence (XRF) core scanning analyses, while the 'working half' was sampled for benthic foraminiferal and dinoflagellate cyst assemblage analyses.

Radiocarbon dates and age model

Nine radiocarbon dates were obtained from calcareous benthic foraminifera found in the core. The material was dated at the AMS Dating Centre at the Institute for Physics and Astronomy, Aarhus University. Data for the samples, reported radiocarbon ages, and calibrated ages are available in Table 1. Radiocarbon dates were calibrated using the Marine13 calibration data set [88] and a marine reservoir age offset ΔR of 139 ± 61 years, following the work of Solignac et al. [112], who based this calculation on the average of several sites around Newfoundland and Labrador in the Marine Reservoir Correction Database [89]. The age-depth model (Fig. 2) was constructed using a P_Sequence depositional model in the age-depth modelling software Oxcal 4.2 [86]. All ages in this paper are listed as calibrated (cal) kyr BP, unless otherwise noted.

Sediment lithology

The lithology of the core was determined through visual sediment description; colours are described according to the Munsell colour chart system. Grain sizes were measured at low resolution on a laser particle sizer at the Vrije Universiteit Amsterdam, the Netherlands (Simon Troelstra and Noortje Dijkstra, *pers. comm.*). These data serve as background information but are not shown here.

Elemental composition

The bulk geochemical composition was determined every centimetre on the split cores using the non-destructive Cortex X-ray fluorescence (XRF) core scanner at Royal NIOZ, the Netherlands [50, 96]. Measurements were taken at 10 kV (Si, Ti, K, Fe and Ca) and 30 kV (Sr) to obtain semi-quantitative abundances of elements and reported as counts per second (cps) (Fig. 3). Elemental abundances were not corrected for sediment accumulation rate.

Foraminiferal assemblages

Samples (1-cm core section) for foraminiferal analyses were taken in 3- to 4-cm intervals through the core. The

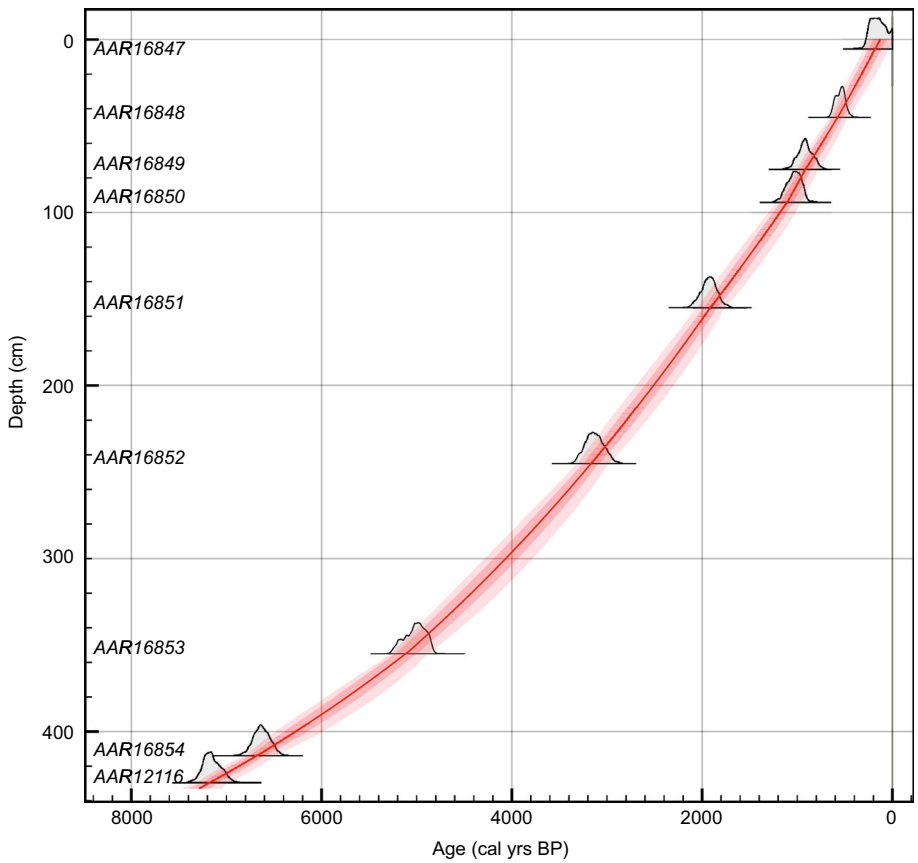

Fig. 2 Age model for core AI07-06G based on radiocarbon dates obtained from foraminifera samples. The *curve* shows the relationship between depth in the core and modelled age, including 1σ (*dark shadow*) and 2σ (*light shadow*) age uncertainties. *Radiocarbon dates* are indicated by their laboratory number and are shown on the *curve* as probability distributions of their calibrated ages. Data for individual radiocarbon dates are found in Table 1

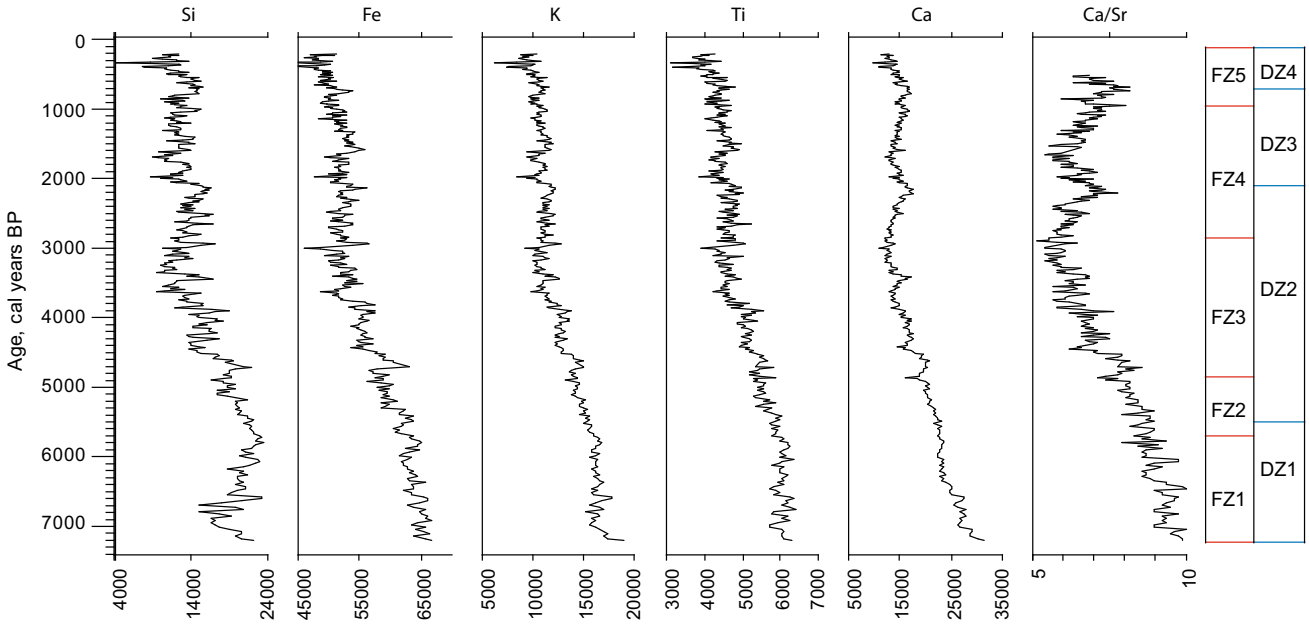

Fig. 3 Results from XRF analyses (presented as counts per seconds) were performed on samples through the core. The *right column* includes the ages of both the foraminiferal and dinoflagellate cyst zones described in this paper. Refer to section "Materials and methods" for details

still wet foraminiferal samples were wet-sieved through sieves with mesh diameters of 1 mm, 100 and 63 µm; the 100-µm to 1-mm fraction was used for the foraminiferal assemblage analysis. To ensure statistical validity of the assemblages, a minimum of 300 individual foraminifera were counted from each sample; if any sample contained

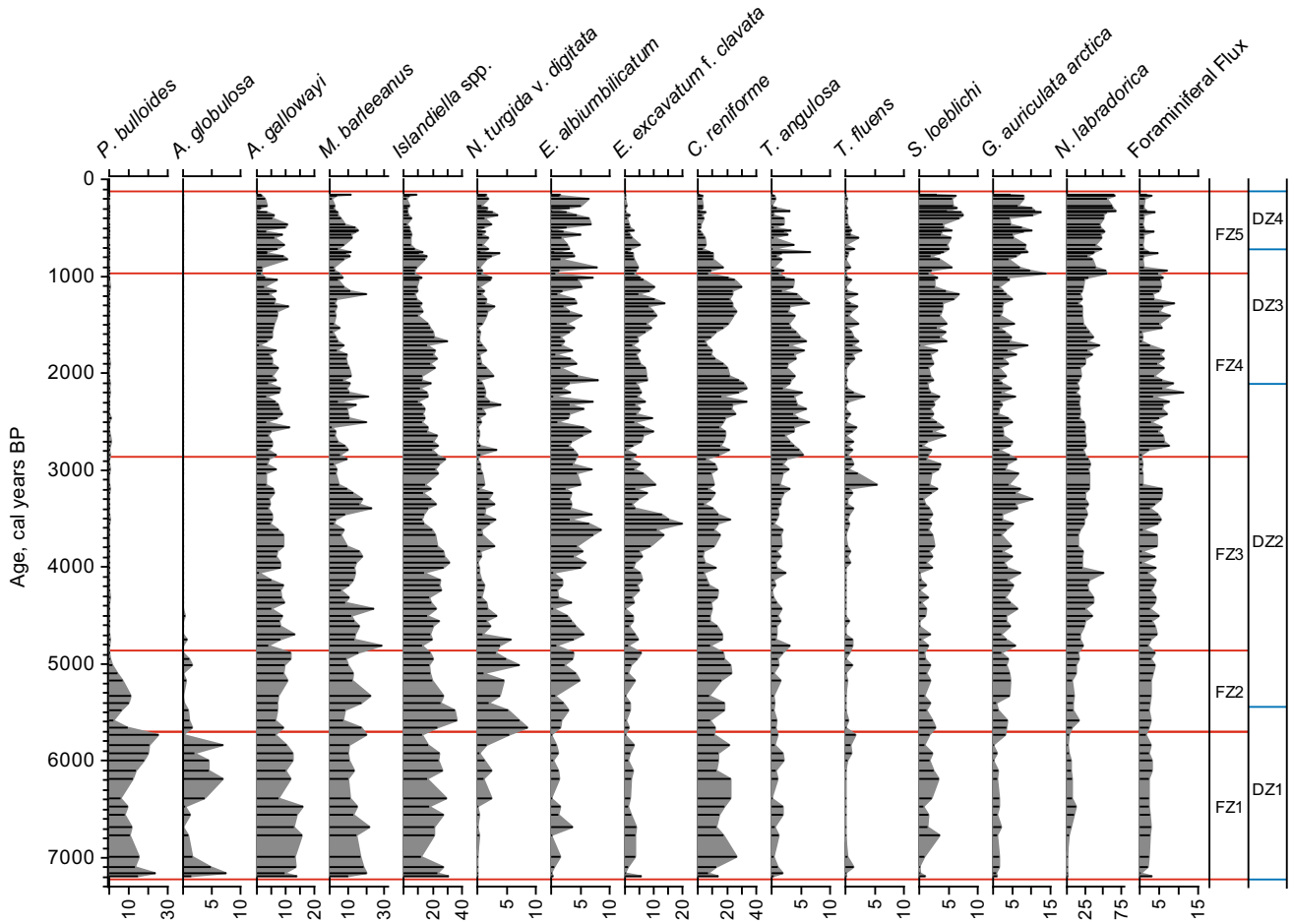

Fig. 4 Benthic foraminiferal assemblages shown in percentages relative to the entire benthic foraminiferal assemblage. The most abundant, and therefore important, species are shown in this figure. Foraminiferal zones are denoted as FZ and were created using cluster analysis results; see section "Materials and methods" for details

insufficient foraminifera, additional sediment was taken from the core at the same sample depth to create a larger sample. Benthic foraminifera were counted and identified down to species level, where possible, to create the faunal assemblages. *Islandiella helenae* and *Islandiella norcrossi* were counted separately but combined in Fig. 4, as samples were counted by several different persons, causing some uncertainty in the precise counts of these species in some of the samples. This did not cause a major loss of information, as the species have quite similar patterns throughout the core; nevertheless, they are in part mentioned separately in the zonal descriptions. The benthic foraminiferal flux was calculated as number of foraminifera per square centimetre of sediment per year (f/cm^2/year), using a sediment density of 1.8 g/cm^3 (cf. [107]). It is worth noting that the core was sampled twice, in 2008 (15 samples) and 2012 (107 samples). Samples processed in 2008 contained higher foraminiferal fluxes than those from 2011, indicating some dissolution after coring, despite the cool room storage of the core. Foraminiferal assemblage compositions were not affected, but the foraminiferal fluxes show some peaks that can be ascribed to the 2008 samples (Fig. 4). The general ecological requirements of the foraminiferal species are discussed in Results; it should be noted that this requires some simplification. A minimum variance, constrained cluster analysis, run on square-root-transformed data, was performed on the foraminiferal assemblage data (Supplementary Figure S1A) using the Multi-Variate Statistics Program (MVSP; [63]).

Dinoflagellate cyst assemblages

Samples for dinoflagellate cyst assemblages were taken in 10-cm intervals for the upper 100 cm of the core, and at 20-cm intervals for the rest of the core. Each sample was spiked with three *Lycopodium* tablets, wrapped in an 11-µm nylon filter, and citric acid was added. The samples were washed for 12 h in a household washing machine at 70 °C and subsequently dried at 50 °C for 48 h. The

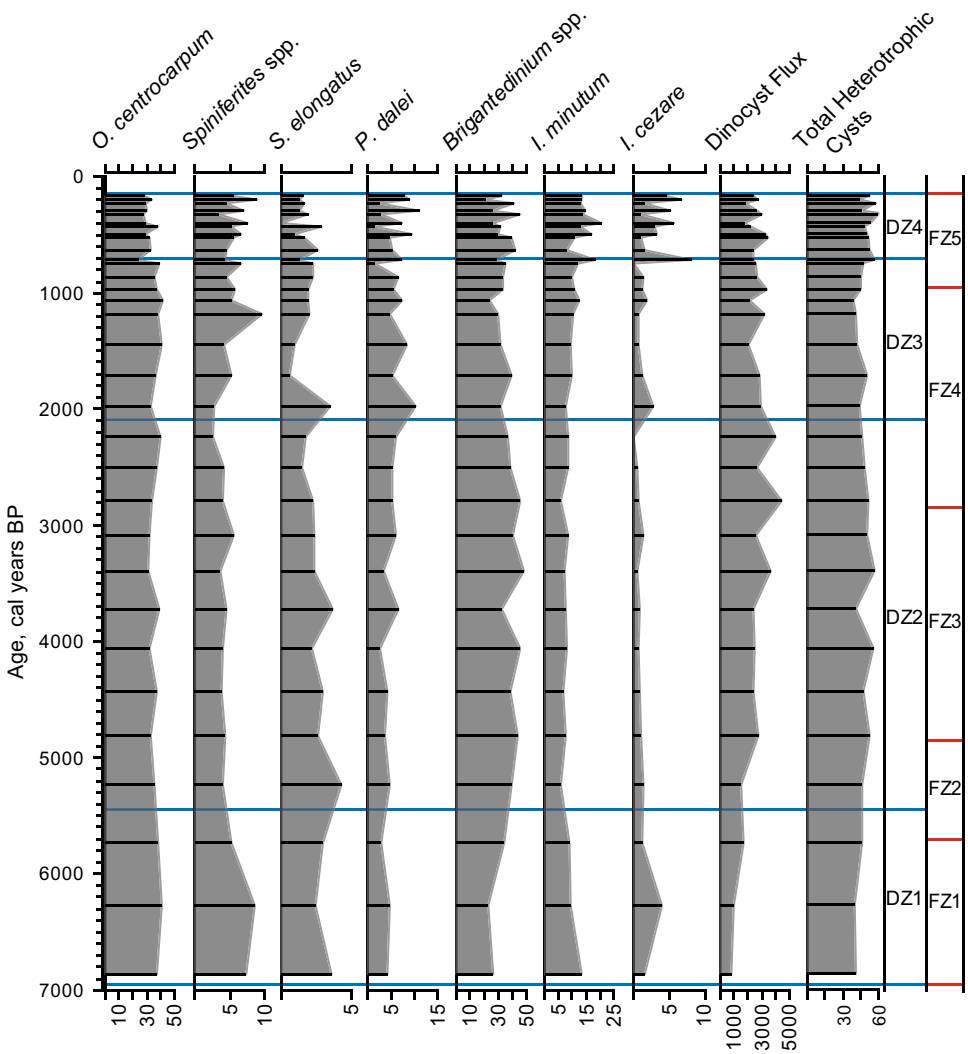

Fig. 5 Assemblages of dinoflagellate cysts shown in percentages relative to the total dinoflagellate cyst assemblage. The most abundant, and therefore important, species and species groups are shown in this figure. Dinoflagellate cyst zones are denoted DZ and were created using cluster analysis results

individual samples were unwrapped and placed into test tubes containing 10 mL of 40 % hydrofluoric acid for 48–72 h, then centrifuged for 3 min at 3000 rpm, and finally, rinsed with distilled water. Samples were prepared for counting by smearing a drop onto a cover slip with a drop of glycerine jelly, dried for 2 h at 50 °C, and finally cooled before counting. In total, 26 samples were analysed with at least 300 dinoflagellate cysts counted in each sample on a transmitted light microscope at 500× magnification and following the taxonomy of Rochon et al. [98] and Head et al. [46]. Here, *Operculodinium centrocarpum* includes both long- and short-process forms of *Operculodinium centrocarpum* sensu Wall and Dale [120] and *Operculodinium centrocarpum*—Arctic morphotype [24]. *Spiniferites elongatus* s.l. includes *Spiniferites elongatus* and *Spiniferites frigidus*, while *Spiniferites* spp. groups unidentifiable and other *Spiniferites* species (i.e. *S. ramosus*, *S. mirabilis*, *S. hyperacanthus*, *S. membranaceus*). *Brigantedinium* spp. includes *Brigantedinium simplex, Brigantedinium cariacoense,* and other round brown spineless cysts that could not be identified at species level. Rare cysts of *Protoperidinium nudum* and *Selenopemphix quanta* were identified at species level but grouped with all other heterotrophic cysts (in Fig. 5). Dinoflagellate cyst flux is defined as number of dinoflagellate cysts per square centimetre of sediment per year (day/cm^2/year). A minimum variance, constrained cluster analysis, run on square-root-transformed data, was performed on the dinoflagellate cyst assemblage data (Supplementary Figure S1B) using the Multi-Variate Statistics Program (MVSP; [63]). In addition, we tested the use of the Modern Analogue Technique (MAT) to make quantitative estimates of past winter and summer sea surface temperature, salinity, and seasonal sea ice cover as described in de Vernal et al. [23], Guiot and de Vernal [41], and de Vernal et al. [26]. However, the MAT analyses resulted in somewhat ambiguous reconstructions and are thus not included in the present study.

The general ecological requirements of the dinoflagellate cyst taxa shown in Fig. 5 are given in Table 3; however, note that such a table may mean some oversimplification.

Results

Age model

The age model shows that the core covers the period from ca. 7.2 cal kyr BP until 0.125 cal kyr BP without any detectable hiatus. Sediment accumulation rates gradually decrease downcore, which may be (partly) due either to compaction or linked to the increasing downward thinning typically seen in gravity cores due to the sediment loss caused by the sediments being pushed laterally outwards ahead of the core tube [39].

Lithology

The sediment of core 06G consists of laminated dark grey/olive grey clay with some fine silt and without visible shell material. Almost all sediment particles are in the clay and silt fractions, with only small amounts of fine sand grains; a few rare particles were present in the coarser 105- to 125-μm fraction (S. Troestra and N. Dijkstra *pers. comm.*), and there is no indication of ice-rafted sediment particles. Grain sizes increase slightly above ~300-cm core depth (ca. 4 cal kyr BP), seen as a very minor increase in the mean sortable silt fraction (not shown). Thin laminations are seen as shifts between slightly lighter and darker bands; no significant change in grain size was linked to these laminations. From 431- to 387-cm core depth (7.2–5.9 cal kyr BP), the clay is very dark grey/olive grey, while laminations are very fine (ca. 0.5 mm), with concentration of lighter and darker laminae giving the appearance of 2- to 4-cm-thick banding with sharp contacts (colour: 5Y 3/1 and 5Y 4/2). The clay sediment of the upper 387 cm of the core (5.9–0.125 cal kyr BP) is somewhat lighter, i.e. dark olive grey and olive grey, with 1- to 6-mm-thick laminations. The laminations are indistinct and discontinuous in the upper 39 cm (0.5–0.125 cal kyr BP), where they are likely disturbed by bioturbation. Occasional worm tubes were observed in the upper 39 cm of the core (colour 5Y 3/1 and 5Y 4/2).

Elemental composition

The X-ray fluorescence (XRF) data from core 06G (Fig. 3) show a general two-part division with a general decrease in the selected elements through time from 7.2 to 3.6 cal kyr BP (431–273 cm), after which the values remained relatively steady. Ca increases again slightly in abundance at ca. 2.3 cal kyr BP (228 cm), also illustrated as a minor increase in the Ca/Sr ratio. The Ca/Sr record does not extend to the very top of the core, as Sr was not measured in the uppermost core section.

Foraminiferal zones

There were very few planktonic foraminifera present in the samples; all are believed to have been transported from the open sea. Due to their very low number, no detailed analyses of the planktonic foraminifera could be carried out. The benthic foraminiferal assemblages were grouped into five foraminiferal assemblage zones (FZ1–FZ5) based on cluster analyses (Fig. 4; S1A).

FZ1 (7.2–5.7 cal kyr BP; 432–379 cm)

This zone contains fairly low foraminiferal fluxes (0.3–3.3 foraminifera/cm^2/year). The main species present in this zone are *Astrononion gallowayi, Melonis barleeanus, Cassidulina reniforme,* and *Islandiella* spp. (slightly more *I. helenae* than *I. norcrossi*), all of which have relatively steady abundances with a few peaks. Peak abundances of *Pullenia bulloides* and *Gyroidina lamarckiana* also characterise this zone. Accessory species encompass *Stainforthia loeblichi*, *Elphidium excavatum* f. *clavata*, *Nonionella turgida* var. *digitata* and *Nonionellina labradorica.* Several of these species, i.e. *P. bulloides, N. turgida* v. *digitata, G. lamarckiana,* and *N. labradorica*, increase in relative abundance in the upper part of the zone, after ca. 6.5 cal kyr BP.

FZ2 (5.7–4.85 cal kyr BP; 379–343 cm)

The foraminiferal flux of this zone is still fairly low (2.3–4.1 f/cm^2/year). The major species in this zone include *A. gallowayi, M. barleeanus, C. reniforme,* and *Islandiella* spp. (mostly *I. helenae*). *P. bulloides* is less abundant in this zone, while *N. turgida* var. *digitata*, *Globobulimina auriculata arctica, N. labradorica,* and *Elphidium albiumbilicatum* increase in abundance. This zone marks the last presence of *P. bulloides* and *G. lamarckiana*.

FZ3 (4.85–2.85 cal kyr BP; 343–224 cm)

The flux in this zone is slightly higher (0.5–5.8 f/cm^2/year) than in FZ2. The main species in this zone are *M. barleeanus, C. reniforme, Islandiella* spp. (mainly *I. helenae), A. gallowayi*, *E. excavatum* f. *clavata* (peaking at ca. 3.7–3.4 cal kyr BP), *N. labradorica, G. auriculata arctica* (upwards increasing), and *E. albiumbilicatum*. Accessory species include *T. angulosa, T. fluens,* and *N.*

turgida var. *digitata*. Notably, a peak in *T. fluens* at ca. 3.2–3.0 cal kyr BP coincides with an interval with low foraminiferal flux.

FZ4 (2.85–0.95 cal kyr BP; 79–224 cm)

The flux in this zone is the highest in the core (0.5–11.3 f/cm^2/year). The main species in this zone include *A. gallowayi, M. barleeanus, C. reniforme*, *Islandiella* spp., *S. loeblichi, G. auriculata arctica, E. albiumbilicatum,* and *N. labradorica,* while *T. angulosa* has its peak abundance in this zone. Accessory species include *I. norcrossi, T. fluens*, and *N. turgida* v. *digitata*. A temporary decrease in the relative abundance of *E. excavatum* f. *clavata*, centred around 1.7 cal kyr BP (140 cm), coincides with a distinct drop in flux and an increase in *N. labradorica* and *G. auriculata arctica*.

FZ5 (0.95–0.49 cal kyr BP; 0–79 cm)

The foraminiferal flux drops to 0.7–7.2 f/cm^2/year (average 1.9 f/cm^2/year). The main species present in this zone include *A. gallowayi, M. barleeanus, Islandiella* spp., *E. albiumbilicatum*, *T. angulosa, S. loeblichi, G. auriculata arctica,* and *N. labradorica,* the latter three increasing in relative abundances in this zone. Accessory species include *C. reniforme, E. excavatum* f. *clavata, T. fluens,* and *N. turgida* v. *digitata*.

Dinoflagellate cyst zones

The dinoflagellate cyst assemblages change very little throughout the core, but could be divided into four dinoflagellate cyst zones (DZ1–4) based on cluster analyses (Fig. 5; S1B):

DZ 1 (7.2–5.45 cal kyr BP; 370–432 cm)

The dinoflagellate cyst flux is the lowest in the core (798–1654 day/cm^2/year), with an average flux of 1144 day/cm^2/year. The most abundant cyst species are *Operculodinium centrocarpum*, *Brigantedinium* spp., and *Islandinium minutum*, while accessory species include *Spiniferites* spp., *Spiniferites elongatus*, cysts of *Pentapharsodinium dalei* (hereafter simply referred to as *P. dalei*) and *Islandinium cezare*.

DZ2 (5.45–2.1 cal kyr BP; 170–370 cm)

The dinoflagellate cyst flux (1477–4508 day/cm^2/year) is generally upwards increasing in this zone, with an average flux of 2904 day/cm^2/year. *O. centrocarpum* continues to be common, as does *Brigantedinium* spp. the latter in slightly higher abundances. Spiniferites spp., *I. minutum* and *I. cezare* are less common, while *S. elongatus* and *P. dalei* have a steady presence, the latter increasing slightly upwards.

DZ3 (2.1–0.71 cal kyr BP; 57–170 cm)

The flux (2039–3411 day/cm^2/year) shows little variability with average values of 2694 day/cm^2/year. The main species in this zone include *Brigantedinium* spp. and *O. centrocarpum*. *I. minutum*, *Spiniferites* spp. and *I. cezare* again increase in this zone. A minor increase is also seen in *P. dalei*.

DZ4 (0.71–0.125 cal kyr BP; 0–57 cm)

The dinoflagellate cyst flux (1744–3486 day/cm^2/year) shows a slight overall decrease, with an average of 2603 day/cm^2/year. *Brigantedinium* spp., and *O. centrocarpum* continue to dominate the assemblage, while *I. minutum*, *Spiniferites* spp., and *I. cezare* continue their increase. *S. elongatus* and *P. dalei* are also still common.

Interpretation

Sediment composition and source

The very dark colour of the sediment and abundant, fine laminations indicate reduced bioturbation and somewhat reduced oxygen levels of the seafloor sediments throughout the core, but especially prior to 5.9 cal kyr BP. The slight increase in grain size and mean sortable silt may be linked to a minor increase in bottom-water energy level, which is in accordance with the more disturbed laminations indicating increased bioturbational activity.

The elemental records for Si, Fe, K, and Ti are interpreted as originating from a terrestrial provenance (see also compilation by [99]). Some sediment may be derived from Newfoundland and transferred to Trinity Bay via the relatively minor riverine run-off; however, the majority is most likely transported from the north with sea ice and icebergs via the Labrador Current, as also previously reported for neighbouring bays by Solignac et al. [112]. Ca is linked to a combination of allochthonous material and local biogenic production, while the Ca/Sr ratio may be considered a proxy for detrital carbonate [49]. The general upward decrease in the elements Si, Fe, K, and Ti observed from 7.2– ca. 3.6 cal kyr BP suggests an upwards decreasing terrestrial input [6, 96, 124], while the small peak in these elements from 4.8 to 4.6 cal kyr BP suggests a temporarily renewed terrestrial input. After ca. 3.6 cal kyr BP, the influx of terrestrial material was relatively stable. The Ca signal may be derived from either

biological productivity or from erosional products, including detrital carbonate. The Ca/Sr ratio, however, suggests that in the early part of the record, a significant part of the Ca was derived from erosional products. This is also supported by the generally low benthic foraminifera flux, a major source of biogenic Ca, in the lower part of the records, compared to the higher foraminiferal fluxes above, especially from ca. 2.8–1.0 cal kyr BP. A similar shift from a dominantly allochthonous to autochthonous source of Ca in the Holocene has also previously been described from other fjords at Newfoundland [112].

Bottom-water conditions based on benthic foraminifera

The calcareous benthic foraminifera were analysed as a proxy for the conditions on the seafloor in Trinity Bay. The basic interpretation of the foraminiferal zones (FZ) is presented here (Fig. 4; Table 2).

7.2–5.7 cal kyr BP (FZ1)

Cold, Arctic-sourced water flushed the seafloor of Trinity Bay (*A. gallowayi, C. reniforme, Islandiella helenae, E. excavatum* f. *clavata*), although some minor influence of warmer water, possibly chilled Atlantic water (*M. barleeanus, I. norcrossi, N. labradorica*), may also be seen. The relatively high abundances of *P. bulloides, M. barleeanus,* and *G. lamarckiana* indicates the presence of buried organic matter and stable conditions; oxygen levels at the seafloor, or at least in the pore water, may have been somewhat reduced at times (*G. auriculata arctica, N. turgida* v. *digitata*), as also supported by the laminated sediment. However, these periods of reduced oxygen content did not severely affect the overall benthic foraminiferal assemblage, indicating a relatively short duration, from a few seasons to a few years. The benthic foraminiferal flux remains fairly low during this period, indicating no large productivity events.

5.7–4.85 cal kyr BP (FZ2)

The dominant species in this zone *C. reniforme, A. gallowayi, Islandiella* spp., and *N. labradorica* suggest an environment with continued dominance of cold Arctic water and a somewhat reduced influx of the influence of Atlantic-sourced water. However, *N. turgida* v. *digitata, N. labradorica,* and *S. loeblichi*, which all thrive in connection to fresh food supply, indicate an increase in primary productivity, possibly linked to a more proximal location of an oceanic front, while *E. albiumbilicatum* suggests a slight reduction in salinity. This may have led to episodes of hypoxic conditions, as indicated by *G. auriculata arctica* and *N. turgida* v. *digitata*, although the less pronounced laminations in the sediment indicate that oxygen levels were generally higher than in zone FZ1.

4.85–2.85 cal kyr BP (FZ3)

The significant influx of *E. excavatum* f. *clavata* and *E. albiumbilicatum* indicates lower bottom-water salinities, in a continued cold-water-dominated environment (*C. reniforme, Islandiella* spp.). A reduction in *M. barleeanus* indicates that the influx of warmer, saline water was at a minimum. Primary production and food supply was still good as indicated by *S. loeblichi, T. fluens, N. labradorica, G. auriculata arctica, N. turgida* v. *digitata* and a high benthic foraminiferal flux, while the decrease in *N. turgida* v. *digitata* indicates that oxygen in the sediments had increased further. This interval is believed to represent a period of freshening of bottom waters.

2.85–0.95 cal kyr BP (FZ4)

The mixture of lower-salinity indicators (*E. excavatum* f. *clavata, E. albiumbilicatum*) and species linked to cold, but more stable, conditions of higher salinity (*C. reniforme*), ventilation of the bottom waters, and increased current activity (*A. gallowayi, T. angulosa*) may be explained by seasonal variability in freshwater flux. Continued high levels of primary productivity (*S. loeblichi, N. labradorica, G. auriculata arctica, N. turgida v. digitata,* high foraminiferal flux) still led to episodes of somewhat reduced oxygen levels that favoured *G. auriculata arctica* and *N. turgida* v. *digitata*. The low foraminiferal flux from 1.7 to 1.5 cal kyr BP coincides with a drop in *C. reniforme* and *E. excavatum* f. *clavata* and peak in productivity and ice edge indicator species *N. labradorica* and *Islandiella* spp. During this interval, there was also a decrease in the low-salinity-tolerant species *E. albiumbilicatum*. A possible link to increased sea ice, which temporarily suppressed foraminiferal productivity, is supported by the presence of the dinoflagellate cyst *I. cezare* (see below; Fig. 5).

0.95–0.13 cal kyr BP (FZ5)

A drop in Arctic (*C. reniforme, Islandiella* spp.) and cold, low-salinity indicators (*E. excavatum* f. *clavata, E. albiumbilicatum*) indicates decreasing influence of the cold, meltwater-bearing LC at the seafloor. This coincides with a significant increase in high-productivity indicators, especially *N. labradorica, S. loeblichi,* and *G. auriculata arctica*. Foraminiferal flux may be artificially low due to dissolution during storage, but even the richest samples (processed in 2008) indicate somewhat reduced flux rates. This may be explained by an environment where high

Table 2 General environmental preferences for benthic foraminifera presented in this paper

Species	Warm species	Cold species	Productivity	Buried organic matter	Meltwater/ low salinity	Tolerates low O2	'Deep' water	Bottom currents	Sea ice cover	References
Astrononion gallowayi		X						X		Rasmussen et al. [87]
Cassidulina reniforme		X								Knudsen et al. [59], Korsun and Hald [62], Lloyd et al. [65], Scott et al. [104]
Elphidium albiumbilicatum					X					Austin and Sejrup [5], Alve [1]
Elphidium excavatum forma *clavata*		X	X							Jennings and Helgadottir [52], Hald and Korsun [42]
Gyroidina lamarckiana			X				X			Finger et al. [34]
Globobulimina auriculata arctica		X		X		X				Corliss [18], Alve and Bernhard [2]
Islandiella helenae		X							X	Hald and Steinsund [43], Steinsund [113], Seidenkrantz [105]
Islandiella norcrossi	X									Steinsund [113], Lloyd [64], Ślubowska-Woldengen et al. [111], Perner et al. [79]
Melonis barleeanus	X		X	X						Caralp [11], Corliss [18], Jennings et al.[53]
Nonionellina labradorica			X						X	Feyling-Hanssen et al. [33], Cedhagen [13], Polyak et al. [82], Jennings et al. [53]
Nonionella turgida var. *digitata*			X			X				Knudsen et al. [61]
Pullenia bulloides		X	X	X						Dijkstra et al. [28]
Stainforthia loeblichi			X						X	Steinsund et al. [114]
Trifarina angulosa								X		Ólafsdóttir et al. [75], Rasmussen et al. [87]
Trifarina fluens		X	X							Rytter et al. [102]

primary productivity could lead to periods of lower pH that may have encouraged calcareous test dissolution. The latter half of the zone saw the lowest abundance of species related to cold water from the LC (*A. gallowayi, C. reniforme, Islandiella* spp.). There is no increase in warmer water species (*M. barleeanus*). The disturbed laminations of the sediment in this zone might indicate increased bioturbation, inferring that the increased productivity did not lead to lowering of bottom-water oxygenation.

Surface water conditions

The dinoflagellate cyst assemblages provide information on the surface water conditions in Trinity Bay. In general, changes in dinoflagellate assemblages are small. However, the assemblages show clear grouping with interval (zones) of comparable assemblages. Similar small, but significant, changes in dinoflagellate cyst assemblages have previously been described from the nearby Bonavista and Placentia Bays [112], indicating that dinoflagellate signals are very subtle in this region despite quite significant (season-specific) changes in environments [110]. In this respect, it should be noted that the cysts in the sediment represent several species, each of which can bloom at a different time of the year; therefore, the dinoflagellate cyst assemblages represent an integration of environmental conditions ranging from early spring to late fall ([117], and references therein). The interpretation is ordered according to dinoflagellate cyst zones (DZ; Fig. 5; Table 3).

7.2–5.5 cal kyr BP (DZ1)

The dominance of *O. centrocarpum* and *Brigantedinium* spp. throughout the core indicates stable seasonal surface water conditions and high nutrient availability over the last ~7.2 kyr. However, this zone is particularly characterised by slightly elevated relative frequencies of *I. minutum* and *I. cezare*, indicating that sea ice was generally present in Trinity Bay for some months every year. The presence of winter sea ice is also supported by the MAT results. The dinoflagellate cyst flux was the lowest in the core, which coincides with the lowest abundances of *Brigantedinium* spp., a genus associated with productivity [37].

5.5–2.1 cal kyr BP (DZ2)

A decrease in *I. minutum* and *I. cezare* indicates a reduction in sea ice cover. This coincided with a steady increase in *Brigantedinium* spp. and dinoflagellate cyst flux, indicating increased nutrients and increased primary production in Trinity Bay (cf. [37]).

2.1–0.71 cal kyr BP (DZ3)

The reintroduction of *I. cezare* and slight increase in *I. minutum* and *P. dalei* suggest that the influx of cold water and seasonal sea ice cover again increased somewhat.

0.71–0.125 cal kyr BP (DZ4)

Sea ice and cold, lower-salinity water influx further increased towards the top of the core (*I. cezare, I. minutum, P. dalei*), causing a slight reduction in sea surface temperatures and reduced, unstable salinities as inferred by the MAT reconstruction. The high nutrient condition continues (dinoflagellate cyst flux).

Discussion

Mid-Holocene

During the Early–Mid-Holocene (ca. 7.2–5.5 cal kyr BP), the dinoflagellate cysts (DZ1) indicate that Trinity Bay was dominated by cold surface waters, most likely sourced from the Arctic via the LC, carrying Polar water south out of Baffin Bay. The presence of *I. cezare* indicates that Trinity Bay experienced seasonal sea ice cover, possibly reflecting the presence of widespread drift ice and icebergs

Table 3 Dinoflagellate cyst species and their associated environmental preferences as compiled from Rochon et al. [98], Marret and Zonneveld [68], and de Vernal et al. [23]

Species	Colder species	Warmer species	Productivity	Sea ice cover
Brigantedinium spp.			X	
Bitectatodinium tepikiense	X			
Cysts of *Pentapharsodinium dalei*	X	X		
Islandinium minutum	X		X	X
Islandinium cezare	X		X	X
Operculodinium centrocarpum	X	X	X	
Spiniferites elongatus	X			
Spiniferites ramosus	X			

entrained by the LC, as also seen today, where ice is carried in winter and spring to the shores of northern Newfoundland. Our study supports the findings of Solignac et al. [112] and Jessen et al. [55], who found cold SSTs around Newfoundland during the Mid-Holocene, ascribing the cause to a stronger than present LC. The increased LC flow may have been caused by stronger atmospheric (westerly wind) circulation patterns [55], combined with high levels of glacial melting in the Arctic. Despite this seasonal transport of sea ice and icebergs from the north, the dinoflagellate cysts indicate that summer sea surface temperatures in Trinity Bay were not particularly cold.

A scenario with a strong LC is also supported by the XRF elemental analysis from core 06G with high values of terrestrial-derived elements (Si, Fe, K, and Ti; Fig. 2). Some of the terrestrial material may have had a local origin, but as Newfoundland was completely deglaciated by 10 cal kyr BP [31] and only small rivers today flow into Trinity Bay, the possibility of transporting sediments of local origin to central Trinity Bay would be limited. Hence, as previously shown by Solignac et al. [112], the relatively high values of K, Fe, and Ti may be largely ascribed to transport of sediments by iceberg and sea ice via the LC, similar to other sediment provenance studies in the North Atlantic region [4, 32]. A significant reduction in meltwater discharge in the Disko area, west Greenland, around 6.0 kyr BP [80] is in support of a strong advection of low-salinity surface water and suspended terrestrial detrital matter prior to 5.5 kyr BP. While both the foraminiferal flux and the dinoflagellate cyst concentrations are relatively low, indicating low biological productivity, the Ca record has high values, indicating that the Early–Mid-Holocene sedimentary record is primarily of allochthonous origin, e.g. from detrital carbonate. This scenario is also supported by the relatively high Ca/Sr ratio (Fig. 3).

In contrast to the ice-loaded surface waters, the water at the seafloor was characterised by high salinities, as evidenced by *P. bulloides, M. barleeanus, A. gallowayi,* and *I. norcrossi*. Despite the common occurrence of *A. gallowayi,* which is often found associated with high bottom-current activity, the dark laminated sediments indicate somewhat reduced bottom-water oxygenation. This may be linked to a stratified water column with higher salinity bottom waters and fresher, ice-influenced surface waters. The presence of *A. gallowayi* may thus be linked to either shorter periods of increased current activity or simply be due to the relatively high salinity of the bottom waters; the latter explanation is supported by the fine-grained sediment and the near absence of other strong current indicators such as *Cibicides* spp. or *Discorbis* spp.

The high-salinity bottom water was likely linked to an influx of Atlantic-sourced water. Two possible sources exist for this Atlantic water: either a northward penetration of the GS into the western sector of the subpolar gyre or a stronger influx of the outer LC with an entrained WGC-derived Atlantic component. Expansion of the GS to the south-west Labrador Sea would mean a significantly northward movement of the LC-GS oceanographic front and the southern margin of the subpolar gyre compared to modern conditions. In a study from Placentia Bay, SE Newfoundland, Sheldon et al. [109] saw no indication of such a strong northward location, and it is thus most likely that the Atlantic water component was derived from the Davis Strait WGC branch [19] entrained by the outer LC.

Our data thus suggest that during the period ca. 7.2–5.5 cal kyr BP, the more saline outer LC penetrated further onto the shelf and into Trinity Bay than it does today, below the relatively low saline, ice-loaded inner LC, which dominated the surface waters of Trinity Bay. This would indicate the presence of a stronger than present subpolar gyre, which allowed a stronger WGC and increased entrainment of the WGC in the LC. A stronger subpolar gyre was also suggested by Sheldon et al. [109] based on foraminiferal data from off SE Newfoundland and is in accordance with the findings by Born and Levermann [9], Gibb et al. [38], Hillaire-Marcel et al. [47], and Seidenkrantz et al. [107]. Also, the timing coincides with the Holocene Thermal Optimum, when a strong northward transport of heat caused increased melting of Arctic glaciers [3, 30, 35]. The Arctic meltwater was transported south by the LC, causing comparatively cold surface water conditions along the east coast of Canada.

After ca. 5.5 cal kyr BP, surface water productivity increased slightly, as reflected in the dinoflagellate cyst flux (DZ2) (Fig. 5). Although sea surface temperatures were still low, the drop in *I. cezare* indicates a reduction in sea ice cover. The concurrent decrease in Ti, Fe, and K (Fig. 3) also supports a decrease in the transport of sediments via sea ice and icebergs from the north. Apart from the episodic presence of (drift) sea ice, laminations in the core sediments could be caused by seasonal changes in water column overturning in the bay and general marine productivity pulses.

Species associated with cold water dominate the foraminiferal faunas. The near disappearance of *P. bulloides* and minor decrease in *C. reniforme,* combined with a minor increase in *E. albiumbilicatum,* indicates increased mixing of the water column with the lower-salinity waters of the inner LC reaching the seafloor. This suggests that the Atlantic water component was reduced, which could have been caused by a weakening of the general subpolar gyre circulation [20], bringing less WGC water to the inner LC reflecting a ceasing inflow of outer LC water into Trinity Bay. At the same time (ca. 5 cal kyr BP), the oceanic front between the LC and GS was shifted

southward, as shown by a decrease in the ocean front indicator *N. labradorica* in Placentia Bay, SE Newfoundland [109]. Although the LC was the dominant water mass influencing Trinity Bay, the decrease in sea ice may be ascribed to a reduction in Arctic glacier melting as also seen later (~4 cal kyr BP) in Bonavista Bay to the north [112]. This was likely caused by the end of the maximum warming of the Holocene Thermal Optimum, resulting in a reduction in Arctic glacier melting [35]. The cold temperatures recorded in Trinity Bay stand in contrast to the generally warmer climate conditions experienced by the western North Atlantic prior to 4 cal kyr BP [21, 25, 58, 67]. However, as also illustrated here, a warmer climate in the Arctic can lead to an increase in glacier melting and thus iceberg export [35], which in turn cools the surface of the LC [55, 93, 110, 112].

Notably, the reduction in meltwater transported south from the Arctic was recorded earlier in Trinity Bay than in Bonavista Bay (after ca. 4 cal kyr BP; [112]) or in Placentia Bay (ca. 2.8 cal kyr BP; [109, 112]). The discrepancy in the timing of the meltwater reduction could be due to a number of factors, including geographical location and current regime. Solignac et al. [112] attributed the continued presence of sea ice in Placentia Bay, with little modern sea ice, to a meridional wind pattern which trapped locally formed sea ice in the fjord until 2.8 cal kyr BP. However, the time lag for the decrease in icebergs between Trinity Bay (~5 kyr PB) and Bonavista Bay to the northwest (~4 kyr BP) is puzzling, but may be due to the fact that the mouth of Bonavista Bay is wider and therefore more open to the Labrador Sea than Trinity Bay. This may have resulted in a trap for icebergs transported with the LC and would have allowed the impact of the, albeit reduced, ice transport to continue influencing the environment of the bay. Satellite images show that today more LC-transported icebergs and sea ice are trapped in Bonavista Bay than in Trinity Bay [74]. This local difference in surface water temperature conditions may therefore be ascribed to the local cooling effect of melting icebergs versus a more general (summer) SST lowering associated with advection of (melting) drift ice and meltwater from the Arctic. Within this context, it may also be relevant to note that a marked reduction in West Greenland inland ice melting has been dated to ca. 3.2 kyr BP [71, 106], indicating a reduction in the production of cold, low-salinity surface water at that time.

Late Holocene

The more unstable conditions and reduction in bottom-water salinity seen after 5 cal kyr BP (increase in foraminiferal species *E. albiumbilicatum* and *E. excavatum* f. *clavata*) may indicate a further reduction in influx of Atlantic-sourced subsurface water from the WGC and increased water column mixing. Furthermore, a decreasing meltwater load within the LC after the Holocene Thermal Optimum (HTO) would have lessened the density gradient between the LC and Atlantic-sourced waters, leading to an increase in water column mixing.

An increase in the duration of the sea ice is evident from the dinoflagellate cyst assemblages after 2.1 cal kyr BP (DZ3), with a further increase in sea ice at ca. 0.7 cal year BP. The sea ice may have facilitated some transport of detrital carbonate as indicated by a slight increase in the Ca/Sr ratio, although the Fe, K, and Ti records indicate little change in sediment provenance. Increased sea ice and the associated increase in nutrients and primary productivity are also supported by the increased frequencies of *S. loeblichi*, which is often found in connection to sea ice [105], and *N. labradorica,* which thrives in high-productivity environments [102]. The continued cold and productive sea surface conditions indicate that the inner LC still strongly influenced the bay. In contrast, Bonavista Bay to the north-west recorded its warmest surface temperatures from 1.7 to 1.1 cal kyr BP [112]. The discrepancy between the bays might be at least partially due to a change in shelf circulation off north-east Newfoundland presumably associated with the regional wind pattern favouring a shift of LC sea ice drift more towards the east. At the same time, this could have been balanced by enhanced outer LC (with entrained WGC Atlantic water) inflow onto the shelf towards the west into Bonavista Bay.

The last 1000 years of the Holocene (zone FZ5 and the top of DZ3 and DZ4; Figs. 4 and 5) represent a cold and productive environment, suggesting that the inner LC was the primary water mass affecting Trinity Bay. However, the presence of *N. labradorica* and *M. barleeanus* suggests continued impact of the WGC also during this time. The drop in foraminiferal species *T. angulosa* may suggest a slight decrease in bottom-current activity. The elemental composition continues to show a decrease in all elements, indicating a lessening of terrestrial input to Trinity Bay, corresponding to the findings of Solignac et al. [112].

The last ca. 0.7 cal kyr BP in Trinity Bay recorded an increase in sea ice and a decrease in surface salinity (Fig. 5). The timing for the start of the cooling corresponds well with the onset of the Little Ice Age [40, 118], but interestingly, the pattern is opposite of that previously described by both Solignac et al. [112] and Sicre et al. [110], who saw a warming of the surface waters in Bonavista Bay. The warmer surface waters off NE Newfoundland have been ascribed to the dominance of the negative phase of the North Atlantic Oscillation (NAO)/Northern Annular Mode (NAM) index [36, 110], which warmed the coastal regions of the Labrador Sea [95, 106, 108, 110]. A negative NAO generally results in less

transport of Arctic water through the Canadian gateway, thus resulting in a weaker LC and associated decreased transport of sea ice during winter and spring. As outlined above, colder conditions in Trinity Bay may well reflect the effect of a changed Little Ice Age atmospheric circulation pattern on the areal distribution of the spring pack ice zone off NE Newfoundland.

The overall cooling of Trinity Bay over the last 2 cal kyr BP is in accordance with the general global-scale cooling of ocean surface temperatures as described by McGregor et al. [69]. The strong millennial-scale variability often seen in the North Atlantic region, overprinting this overall cooling [54, 57, 60, 91, 92, 106, 110, 116], is not strongly recorded in Trinity Bay. This may be due to either a lower sensitivity of the proxies to such relatively minor variations in the environment, or to the relatively enclosed setting of Trinity Bay. The narrow inlet may provide optimal entry for cold inner LC waters while the bulk of the outer LC, with its entrained WGC component, misses the bay.

Conclusions

The Early–Mid-Holocene in Trinity Bay was characterised by cold conditions at the surface, controlled by the inner Labrador Current (LC), and relatively high salinities at the seafloor, possibly due to the presence of Atlantic-sourced water from the West Greenland Current (WGC). The subpolar gyre was likely stronger during this period, allowing more WGC-derived Atlantic water to reach the western side of the Labrador Sea. There is a clear presence of sea ice in Trinity Bay at this time, likely entrained by the LC out of the Canadian Arctic archipelago and Baffin Bay. During this time, the warmer climate in the Arctic led to increasing glacier melting and release of icebergs, increasing the abundance of icebergs originating from the Baffin Bay-bordering outlet glaciers.

Following this, the water column in the bay became more mixed and productivity increased. Sea ice became less prevalent in the bay during the Late Holocene, which could be linked to a decrease in Arctic-sourced meltwater, sea ice, and icebergs transported by the LC. This could also be linked to a weaker subpolar gyre, implying less entrainment of WGC Atlantic-derived water along the western side of the subpolar gyre. The Late Holocene thus experienced a cold and productive environment in the bay, mainly characterised by the inner LC. The end of the Holocene saw a gradual shift into modern conditions, with a dominantly cold water mass sourced from the inner LC and some influence from warmer Atlantic waters entrained in the outer LC.

The climate over the last 7200 years of the western Labrador Sea region has been strongly influenced by the strength of the LC, which, together with the regional atmospheric circulation pattern, has had a marked impact on the local fjord environment of northern Newfoundland. Smaller changes in the main pattern of sea ice and iceberg drift related to regional ocean and atmospheric circulation variations are concluded to have had well-defined, but different effects on the various fjords here.

Acknowledgments We would like to thank the captain and crew of RV 'Akademik Ioffe', as well as the entire scientific party for their help during the research cruise. We thank Kirsten Rosendal for her help with dinoflagellate cyst laboratory preparations. We are also grateful to Simon Troelstra and Noortje Dijkstra, Vrije Universiteit Amsterdam, the Netherlands, for placing low-resolution grain size data at our disposal. We would also like to thank the anonymous reviewers and the journal editor for the constructive comments and suggestions.

Funding This study was funded by 'Kommisionen for Videnskabelige Undersøgelser i Grønland', the Danish Council for Independent Research, Natural Science (project nos. 12-126709/FNU, DFF-4002-00098_FNU) and the European Union's Seventh Framework programme (FP7/2007-2013) under Grant Agreement No. 243908, 'Past4Future, Climate change—Learning from the past climate'. The cruise was funded by the Danish Council for Independent Research, Natural Science (Project No. 272-06-0604/FNU) and carried out within the Danish–Russian collaboration project 'Joint paleoceanographic investigations in the Labrador Sea region'.

References

1. Alve E (1995) Benthic foraminiferal distribution and recolonization of formerly anoxic environments in Drammensfjord, southern Norway. Mar Micropaleontol 25:169–186. doi:10.1016/0377-8398(95)00007-N
2. Alve E, Bernhard J (1995) Vertical migratory response of benthic foraminifera to controlled oxygen concentrations in an experimental mesocosm. Mar Ecol Prog Ser 116:137–151. doi:10.3354/meps116137
3. Andersen C, Koç N, Moros M (2004) A highly unstable Holocene climate in the subpolar North Atlantic: evidence from diatoms. Quat Sci Rev 23:2155–2166. doi:10.1016/j.quascirev.2004.08.004
4. Andrews JT (2000) Icebergs and iceberg rafted detritus (IRD) in the North Atlantic: facts and assumptions. Oceanography 13:100–108. doi:10.5670/oceanog.2000.19
5. Austin WEN, Sejrup HP (1994) Recent shallow water benthic foraminifera from western Norway: ecology and palaeoecological significance. Cushman Found Spec Publ 32:103–125
6. Bahr A, Lamy F, Arz H et al (2005) Late glacial to Holocene climate and sedimentation history in the NW Black Sea. Mar Geol 214:309–322. doi:10.1016/j.margeo.2004.11.013
7. Banfield CE (1983) Climate (Newfoundland). In: South JR (ed) Biogeography and ecology of the island of Newfoundland. W. Junk, The Hague, pp 37–106
8. Böning CW, Scheinert M, Dengg J et al (2006) Decadal variability of subpolar gyre transport and its reverberation in the

North Atlantic overturning. Geophys Res Lett 33:L21S01. doi:10.1029/2006GL026906
9. Born A, Levermann A (2010) The 8.2ka event: abrupt transition of the subpolar gyre toward a modern North Atlantic circulation. Geochem Geophys Geosystems 11:Q06011. doi:10.1029/2009GC003024
10. Canadian Ice Service (2013) Climatic Ice Atlas 1981–2010 [online]. http://www.ec.gc.ca/glaces-ice
11. Caralp MH (1989) Abundance of Bulimina exilis and Melonis barleeanum: relationship to the quality of marine organic matter. Geo Mar Lett 9:37–42. doi:10.1007/BF02262816
12. Catto NR, Hooper RG, Anderson MR et al (1999) Biological and geomorphological classification of Placentia Bay: a preliminary assessment. Can Tech Rept Fish Aquat Sci 2289:35
13. Cedhagen T (1991) Retention of chloroplasts and bathymetric distribution in the sublittoral foraminiferan Nonionellina labradorica. Ophelia 33:17–30. doi:10.1080/00785326.1991.10429739
14. Clarke RA, Gascard J-C (1983) The formation of Labrador Sea water. Part I: large-scale processes. J Phys Oceanogr 13:1764–1778. doi:10.1175/1520-0485(1983)013%3C1764:TFOLSW%3E2.0.CO;2
15. Clark PU, Marshall SJ, Clarke GKC et al (2001) Freshwater forcing of abrupt climate change during the last glaciation. Science 293:283–287. doi:10.1126/science.1062517
16. Clark PU, Pisias NG, Stocker TF, Weaver AJ (2002) The role of the thermohaline circulation in abrupt climate change. Nature 415:863–869. doi:10.1038/415863a
17. Colbourne E, Senciall DR (1993) Temperature, salinity and density along the standard Bonavista transect. Can Tech Rep Hydrogr Ocean Sci 150:331
18. Corliss B (1991) Morphology and microhabitat preferences of benthic foraminifera from the northwest Atlantic Ocean. Mar Micropaleontol 17:195–236. doi:10.1016/0377-8398(91)90014-W
19. Cuny J, Rhines PB, Niiler PP, Bacon S (2002) Labrador Sea boundary currents and the fate of the Irminger Sea Water. J Phys Oceanogr 32:627–647. doi:10.1175/1520-0485(2002)032<0627:LSBCAT>2.0.CO;2
20. Curry R, McCartney M (2001) Ocean gyre circulation changes associated with the North Atlantic Oscillation. J Phys Oceanogr 31:3374–3400. doi:10.1175/1520-0485(2001)031<3374:OGCCAW>2.0.CO;2
21. Dahl-Jensen D (1998) Past temperatures directly from the Greenland Ice Sheet. Science 282:268–271. doi:10.1126/science.282.5387.268
22. Deser C, Holland M, Reverdin G, Timlin M (2002) Decadal variations in Labrador Sea ice cover and North Atlantic sea surface temperatures. J Geophys Res 107:3–1–3–12. doi:10.1029/2000JC000683
23. de Vernal A, Eynaud F, Henry M et al (2005) Reconstruction of sea-surface conditions at middle to high latitudes of the Northern Hemisphere during the Last Glacial Maximum (LGM) based on dinoflagellate cyst assemblages. Quat Sci Rev 24:897–924. doi:10.1016/j.quascirev.2004.06.014
24. de Vernal A, Henry M, Matthiessen J et al (2001) Dinoflagellate cyst assemblages as tracers of sea-surface conditions in the northern North Atlantic, Arctic and sub-Arctic seas: the new "n = 677" data base and its application for quantitative palaeoceanographic reconstruction. J Quat Sci 16:681–698. doi:10.1002/jqs.659
25. de Vernal A, Hillaire-Marcel C (2006) Provincialism in trends and high frequency changes in the northwest North Atlantic during the Holocene. Glob Planet Change 54:263–290. doi:10.1016/j.gloplacha.2006.06.023
26. de Vernal A, Rochon A, Fréchette B et al (2013) Reconstructing past sea ice cover of the Northern Hemisphere from dinocyst assemblages: status of the approach. Quat Sci Rev 79:122–134. doi:10.1016/j.quascirev.2013.06.022
27. de Young B, Sanderson B (1995) The circulation and hydrography of Conception Bay, Newfoundland. Atmos Ocean 33:135–162. doi:10.1080/07055900.1995.9649528
28. Dijkstra N, Junttila J, Carroll J et al (2013) Baseline benthic foraminiferal assemblages and habitat conditions in a sub-Arctic region of increasing petroleum development. Mar Environ Res 92:178–196. doi:10.1016/j.marenvres.2013.09.014
29. Drinkwater K (1996) Atmospheric and oceanic variability in the Northwest Atlantic during the 1980s and early 1990s. J Northwest Atl Fish Sci 18:77–97. doi:10.2960/J.v18.a6
30. Duplessy J-C, Ivanova E, Murdmaa I et al (2001) Holocene paleoceanography of the northern Barents Sea and variations of the northward heat transport by the Atlantic Ocean. Boreas 30:2–16. doi:10.1111/j.1502-3885.2001.tb00984.x
31. Dyke A (2004) An outline of North American deglaciation with emphasis on central and northern Canada. Dev Quat Sci 2:373–424. doi:10.1016/S1571-0866(04)80209-4
32. Farmer GL, Barber D, Andrews J (2003) Provenance of Late Quaternary ice-proximal sediments in the North Atlantic: Nd, Sr and Pb isotopic evidence. Earth Planet Sci Lett 209:227–243. doi:10.1016/S0012-821X(03)00068-2
33. Feyling-Hanssen RW, Jorgensen JA, Knudsen KL, Andersen A-LL (1971) Later Quaternary foraminifera from Vensyssel, Denmark and Sandnes, Norway. In: Bulletin of the Geological Society of Denmark, pp 67–317
34. Finger K, Encinas A, Nielsen S, Peterson D (2003) Microfaunal indications of late Miocene deep-water basins off the central coast of Chile. Concepción, Chile
35. Fisher DA, Koerner RM, Reeh N (1995) Holocene climatic records from Agassiz Ice Cap, Ellesmere Island, NWT, Canada. The Holocene 5:19–24. doi:10.1177/095968369500500103
36. Frankignoul C, de Coëtlogon G, Joyce TM, Dong S (2001) Gulf stream variability and Ocean-Atmosphere Interactions. J Phys Oceanogr 31:3516–3529. doi:10.1175/1520-0485(2002)031<3516:GSVAOA>2.0.CO;2
37. Gaines G, Elbrächter M (1987) Chapter 6: Heterotrophic nutrition. The biology of dinoflagellates. Blackwell Scientific Publications, Oxford, pp 224–268
38. Gibb OT, Hillaire-Marcel C, de Vernal A (2013) Oceanographic regimes in the northwest Labrador Sea since Marine Isotope Stage 3 based on dinocyst and stable isotope proxy records. Quat Sci Rev 92:269–279. doi:10.1016/j.quascirev.2013.12.010
39. Glew J, Smol J, Last W (2001) Sediment Core Collection and Extrusion. In: Last W, Smol J (eds) Tracking environmental change using lake sediments. Springer, The Netherlands, pp 73–105
40. Grove JM (2001) The initiation of the "Little Ice Age" in regions round the North Atlantic. In: Ogilvie AJ, Jónsson T (eds) The iceberg in the mist: Northern research in pursuit of a "Little Ice Age". Springer, The Netherlands, pp 53–82
41. Guiot J, de Vernal A (2007) Chapter thirteen transfer functions: methods for quantitative paleoceanography based on microfossils. In: Developments in marine geology. Elsevier, New York, pp 523–563
42. Hald M, Korsun S (1997) Distribution of modern benthic foraminifera from fjords of Svalbard, European Arctic. J Foraminifer Res 27:101–122. doi:10.2113/gsjfr.27.2.101
43. Hald M, Steinsund PI (1992) Distribution of surface sediment benthic foraminifera in the southwestern Barents Sea. J Foraminifer Res 22:347–362. doi:10.2113/gsjfr.22.4.347
44. Han G, Lu Z, Wang Z et al (2008) Seasonal variability of the Labrador Current and shelf circulation off Newfoundland. J Geophys Res 113:C10013. doi:10.1029/2007JC004376

45. Hátún H, Sandø AB, Drange H et al (2005) Influence of the Atlantic Subpolar Gyre on the thermohaline circulation. Science 309:1841–1844. doi:10.1126/science.1114777
46. Head MJ, Harland R, Matthiessen J (2001) Cold marine indicators of the late quaternary: the new dinoflagellate cyst genus Islandinium and related morphotypes. J Quat Sci 16:621–636. doi:10.1002/jqs.657
47. Hillaire-Marcel C, de Vernal A, Bilodeau G, Weaver A (2001) Absence of deep-water formation in the Labrador Sea during the last interglacial period. Nature 410:1073–1077. doi:10.1038/35074059
48. Hillaire-Marcel C, Maccali J, Not C, Poirier A (2013) Geochemical and isotopic tracers of Arctic sea ice sources and export with special attention to the Younger Dryas interval. Quat Sci Rev 79:184–190. doi:10.1016/j.quascirev.2013.05.001
49. Hodell DA, Channell JET, Curtis JH et al (2008) Onset of "Hudson Strait" Heinrich events in the eastern North Atlantic at the end of the middle Pleistocene transition (~640 ka)? Paleoceanography 23:PA4218. doi:10.1029/2008PA001591
50. Jansen JH, Van der Gaast S, Koster B, Vaars A (1998) CORTEX, a shipboard XRF-scanner for element analyses in split sediment cores. Mar Geol 151:143–153. doi:10.1016/S0025-3227(98)00074-7
51. Jennings AE, Andrews J, Pearce C et al (2015) Detrital carbonate peaks on the Labrador shelf, a 13–7 ka template for freshwater forcing from the Hudson Strait outlet of the Laurentide Ice Sheet into the subpolar gyre. Quat Sci Rev 107:62–80. doi:10.1016/j.quascirev.2014.10.022
52. Jennings AE, Helgadottir G (1994) Foraminiferal assemblages from the fjords and shelf of eastern Greenland. J Foraminifer Res 24:123–144. doi:10.2113/gsjfr.24.2.123
53. Jennings AE, Weiner NJ, Helgadottir G, Andrews JT (2004) Modern foraminiferal faunas of the southwestern to northern Iceland shelf: oceanographic and environmental controls. J Foraminifer Res 34:180–207. doi:10.2113/34.3.180
54. Jessen CA, Rundgren M, Björck S, Hammarlund D (2005) Abrupt climatic changes and an unstable transition into a late Holocene Thermal Decline: a multiproxy lacustrine record from southern Sweden. J Quat Sci 20:349–362. doi:10.1002/jqs.921
55. Jessen CA, Solignac S, Nørgaard-Pedersen N et al (2011) Exotic pollen as an indicator of variable atmospheric circulation over the Labrador Sea region during the mid to late Holocene. J Quat Sci 26:286–296. doi:10.1002/jqs.1453
56. Katsman CA, Spall MA, Pickart RS (2004) Boundary current eddies and their role in the restratification of the Labrador Sea. J Phys Oceanogr 34:1967–1983. doi:10.1175/1520-0485(2004)034<1967:BCEATR>2.0.CO;2
57. Kaufman DS, Ager TA, Anderson NJ et al (2004) Holocene thermal maximum in the western Arctic (0–180°W). Quat Sci Rev 23:529–560. doi:10.1016/j.quascirev.2003.09.007
58. Keigwin LD, Sachs JP, Rosenthal Y, Boyle EA (2005) The 8200 year B.P. event in the slope water system, western subpolar North Atlantic. Paleoceanography 20:PA2003. doi:10.1029/2004PA001074
59. Knudsen KL, Conradsen K, Heier-Nielsen S, Seidenkrantz MS (1996) Palaeoenvironments in the Skagerrak–Kattegat basin in the eastern North Sea during the last deglaciation. Boreas 25:65–78. doi:10.1111/j.1502-3885.1996.tb00836.x
60. Knudsen KL, Søndergaard MKB, Eiríksson J, Jiang H (2008) Holocene thermal maximum off North Iceland: evidence from benthic and planktonic foraminifera in the 8600–5200 cal year BP time slice. Mar Micropaleontol 67:120–142. doi:10.1016/j.marmicro.2007.11.003
61. Knudsen KL, Stabell B, Seidenkrantz M-S et al (2008) Deglacial and Holocene conditions in northernmost Baffin Bay: sediments, foraminifera, diatoms and stable isotopes. Boreas 37:346–376. doi:10.1111/j.1502-3885.2008.00035.x
62. Korsun S, Hald M (2000) Seasonal dynamics of benthic foraminifera in a glacially fed fjord of Svalbard, European Arctic. J Foraminifer Res 30:251–271. doi:10.2113/0300251
63. Kovach WL (1998) Multi-variate statistical package. Kovach Computing Services, Pentraeth, Wales
64. Lloyd JM (2006) Late Holocene environmental change in Disko Bugt, west Greenland: interaction between climate, ocean circulation and Jakobshavn Isbrae. Boreas 35:35–49. doi:10.1111/j.1502-3885.2006.tb01111.x
65. Lloyd JM, Park LA, Kuijpers A, Moros M (2005) Early Holocene palaeoceanography and deglacial chronology of Disko Bugt, West Greenland. Quat Sci Rev 24:1741–1755. doi:10.1016/j.quascirev.2004.07.024
66. Locarnini RA, Mishonov AV, Antonov JI et al (2013) World Ocean Atlas 2013, Volume 1: temperature. NOAA Atlas NESDIS 73:40
67. MacPherson J (1995) A 6 ka BP reconstruction for the island of Newfoundland from a synthesis of Holocene lake-sediment pollen records. Géographie Phys Quat 49:163–182. doi:10.7202/033035ar
68. Marret F, Zonneveld KAF (2003) Atlas of modern organic-walled dinoflagellate cyst distribution. Rev Palaeobot Palynol 125:1–200. doi:10.1016/S0034-6667(02)00229-4
69. McGregor H, Evans MN, Goosse H et al (2015) Robust global ocean cooling trend for the pre-industrial Common Era. Nat Geosci 8:671–677. doi:10.1038/ngeo2510
70. Mertz G, Narayanan S, Helbig J (1993) The freshwater transport of the labrador current. Atmos Ocean 31:281–295. doi:10.1080/07055900.1993.9649472
71. Møller HS, Jensen KG, Kuijpers A et al (2006) Late-Holocene environment and climatic changes in Ameralik Fjord, southwest Greenland: evidence from the sedimentary record. Holocene 16:685–695. doi:10.1191/0959683606hl963rp
72. Myers PG (2005) Impact of freshwater from the Canadian Arctic Archipelago on Labrador Sea Water formation. Geophys Res Lett. doi:10.1029/2004GL022082
73. Narayanan S, Colboume EB, Fitzpatrick C (1991) Frontal oscillations on the NE Newfoundland shelf. Atmos Ocean 29:547–562. doi:10.1080/07055900.1991.9649416
74. NSIDC (2015) National Snow and Ice Data Center. In: Arct. Sea Ice News Anal. http://nsidc.org/arcticseaicenews/
75. Ólafsdóttir S, Jennings AE, Geirsdóttir Á et al (2010) Holocene variability of the North Atlantic Irminger current on the south- and northwest shelf of Iceland. Mar Micropaleontol 77:101–118. doi:10.1016/j.marmicro.2010.08.002
76. Parrish CC (1998) Lipid biogeochemistry of plankton, settling matter and sediments in Trinity Bay. Newfoundland. I. Lipid classes. Org Geochem 29:1531–1545. doi:10.1016/S0146-6380(98)00176-4
77. Pearce C, Seidenkrantz M-S, Kuijpers A et al (2013) Ocean lead at the termination of the Younger Dryas cold spell. Nat Commun 4:1664. doi:10.1038/ncomms2686
78. Pearce C, Seidenkrantz M-S, Kuijpers A, Reynisson NF (2014) A multi-proxy reconstruction of oceanographic conditions around the Younger Dryas-Holocene transition in Placentia Bay, Newfoundland. Mar Micropaleontol 112:39–49. doi:10.1016/j.marmicro.2014.08.004
79. Perner K, Moros M, Lloyd JM et al (2011) Centennial scale benthic foraminiferal record of late Holocene oceanographic variability in Disko Bugt, West Greenland. Quat Sci Rev 30:2815–2826. doi:10.1016/j.quascirev.2011.06.018
80. Perner K, Moros M, Snowball I et al (2013) Establishment of modern circulation pattern at c. 6000 cal a BP in Disko Bugt, central West Greenland: opening of the Vaigat Strait. J Quat Sci 28:480–489. doi:10.1002/jqs.2638

81. Petrie B (2007) Does the north Atlantic oscillation affect hydrographic properties on the Canadian Atlantic continental shelf? Atmos Ocean 45:141–151. doi:10.3137/ao.450302
82. Polyak L, Korsun S, Febo LA et al (2002) Benthic foraminiferal assemblages from the southern Kara Sea, a river-influenced Arctic marine environment. J Foraminifer Res 32:252–273. doi:10.2113/32.3.252
83. Prinsenberg SJ, Peterson IK, Narayanan S, Umoh JU (1997) Interaction between atmosphere, ice cover, and ocean off Labrador and Newfoundland from 1962 to 1992. Can J Fish Aquat Sci 54:30–39. doi:10.1139/f96-150
84. Rahmstorf S (1996) On the freshwater forcing and transport of the Atlantic thermohaline circulation. Clim Dyn 12:799–811. doi:10.1007/s003820050144
85. Rahmstorf S (2006) Thermohaline Ocean circulation. Encycl Quat, Sci
86. Ramsey CB (2008) Deposition models for chronological records. Quat Sci Rev 27:42–60. doi:10.1016/j.quascirev.2007.01.019
87. Rasmussen TL, Thomsen E, Nielsen T, Wastegård S (2011) Atlantic surface water inflow to the Nordic seas during the Pleistocene-Holocene transition (mid-late Younger Dryas and Pre-Boreal periods, 12 450–10 000 a BP). J Quat Sci 26:723–733. doi:10.1002/jqs.1496
88. Reimer P, Bard E, Bayliss A et al (2013) IntCal13 and Marine13 radiocarbon age calibration curves 0–50,000 years cal BP. Radiocarbon 55:1869–1887. doi:10.2458/azu_js_rc.55.16947
89. Reimer PJ, Reimer RW (2001) A marine reservoir correction database and on-line interface. Radiocarbon 43:461–463
90. Ren J, Jiang H, Seidenkrantz M-S, Kuijpers A (2009) A diatom-based reconstruction of Early Holocene hydrographic and climatic change in a southwest Greenland fjord. Mar Micropaleontol 70:166–176. doi:10.1016/j.marmicro.2008.12.003
91. Renssen H, Seppä H, Crosta X et al (2012) Global characterization of the Holocene thermal maximum. Quat Sci Rev 48:7–19. doi:10.1016/j.quascirev.2012.05.022
92. Renssen H, Seppä H, Heiri O et al (2009) The spatial and temporal complexity of the Holocene thermal maximum. Nat Geosci 2:411–414. doi:10.1038/ngeo513
93. Reverdin G, Cayan D, Kushnir Y (1997) Decadal variability of hydrography in the upper northern North Atlantic in 1948–1990. J Geophys Res 102:8505–8531. doi:10.1029/96JC03943
94. Rhein M, Kieke D, Hüttl-Kabus S et al (2011) Deep water formation, the subpolar gyre, and the meridional overturning circulation in the subpolar North Atlantic. Deep Sea Res Part II Top Stud Oceanogr 58:1819–1832. doi:10.1016/j.dsr2.2010.10.061
95. Ribeiro S, Moros M, Ellegaard M, Kuijpers A (2011) Climate variability in West Greenland during the past 1500 years: evidence from a high-resolution marine palynological record from Disko Bay: climate variability in West Greenland during the past 1500 years. Boreas 41:68–83. doi:10.1111/j.1502-3885.2011.00216.x
96. Richter TO, van der Gaast S, Koster B et al (2006) The Avaatech XRF Core Scanner: technical description and applications to NE Atlantic sediments. Geol Soc Lond Spec Publ 267:39–50. doi:10.1144/GSL.SP.2006.267.01.03
97. Robe RQ, Maier DC, Russell WE (1980) Long-term drift of icebergs in Baffin Bay and the Labrador Sea. Cold Reg Sci Technol 1:183–193. doi:10.1016/0165-232X(80)90047-6
98. Rochon A, de Vernal A, Turon JL et al (1999) Distribution of recent dinoflagellate cysts in surface sediments from the North Atlantic Ocean and adjacent seas in relation to sea-surface parameters. Am Assoc Stratigr Palynol Contrib Ser 35:1–146
99. Rothwell RG, Croudace IW (2015) Twenty years of XRF core scanning marine sediments: What do geochemical proxies tell us? In: Croudace IW, Rothwell RG (eds) Micro-XRF studies of sediment cores. Springer, Dordrecht, The Netherlands, pp 25–102
100. Rudels B (1995) The thermohaline circulation of the Arctic Ocean and the Greenland Sea. Philos Trans R Soc Math Phys Eng Sci 352:287–299. doi:10.1098/rsta.1995.0071
101. Rudels B, Quadfasel D (1991) Convection and deep water formation in the Arctic Ocean-Greenland Sea system. J Mar Syst 2:435–450. doi:10.1016/0924-7963(91)90045-V
102. Rytter F, Knudsen KL, Seidenkrantz M-S, Eiríksson J (2002) Modern distribution of benthic foraminifera on the North Icelandic shelf and slope. J Foraminifer Res 32:217–244. doi:10.2113/32.3.217
103. Schillinger DJ, De Young B, Foley JS (2000) Tow-yo and temperature data from Trinity Bay, May 2000. Dept. of Physics and Physical Oceanography, Memorial University of Newfoundland
104. Scott DB, Schell T, Rochon A, Blasco S (2008) Benthic foraminifera in the surface sediments of the Beaufort Shelf and slope, Beaufort Sea, Canada: applications and implications for past sea-ice conditions. J Mar Syst 74:840–863. doi:10.1016/j.jmarsys.2008.01.008
105. Seidenkrantz M-S (2013) Benthic foraminifera as palaeo sea-ice indicators in the subarctic realm—examples from the Labrador Sea-Baffin Bay region. Quat Sci Rev 79:135–144. doi:10.1016/j.quascirev.2013.03.014
106. Seidenkrantz M-S, Aagaard-Sørensen S, Sulsbrück H et al (2007) Hydrography and climate of the last 4400 years in a SW Greenland fjord: implications for Labrador Sea palaeoceanography. Holocene 17:387–401. doi:10.1177/0959683607075840
107. Seidenkrantz M-S, Ebbesen H, Aagaard-Sørensen S et al (2013) Early Holocene large-scale meltwater discharge from Greenland documented by foraminifera and sediment parameters. Palaeogeogr Palaeoclimatol Palaeoecol 391:71–81. doi:10.1016/j.palaeo.2012.04.006
108. Seidenkrantz M-S, Roncaglia L, Fischel A et al (2008) Variable North Atlantic climate seesaw patterns documented by a late Holocene marine record from Disko Bugt, West Greenland. Mar Micropaleontol 68:66–83. doi:10.1016/j.marmicro.2008.01.006
109. Sheldon CM, Pearce C, Seidenkrantz M-S et al (2015) Holocene oceanographic changes in Placentia Bay, Newfoundland. The Holocene. doi:10.1177/0959683615608690
110. Sicre M-A, Weckström K, Seidenkrantz M-S et al (2014) Labrador current variability over the last 2000 years. Earth Planet Sci Lett 400:26–32. doi:10.1016/j.epsl.2014.05.016
111. Ślubowska-Woldengen M, Rasmussen TL, Koç N et al (2007) Advection of Atlantic Water to the western and northern Svalbard shelf since 17,500 cal yr BP. Quat Sci Rev 26:463–478. doi:10.1016/j.quascirev.2006.09.009
112. Solignac S, Seidenkrantz MS, Jessen C et al (2011) Late–Holocene sea-surface conditions offshore Newfoundland based on dinoflagellate cysts. Holocene 21:539–552. doi:10.1177/0959683610385720
113. Steinsund PI (1994) Benthic Foraminifera in surface sediments of the Barents and Kara Seas: Modern and Late Quaternary Applications. Doctor Scientiarum thesis, University of Tromsø
114. Steinsund PI, Polyak L, Hald M et al (1994) Distribution of calcareous benthic foraminifera in recent sediments of the Barents and Kara Sea. In: Benthic Foraminifera in surface sediments of the Barents and Kara Seas: modern and late quaternary application. Department of Geology, Institute of Biology and Geology, University of Tromsø, Norway
115. Talley LD, McCartney MS (1982) Distribution and circulation of Labrador Sea Water. J Phys Oceanogr 12:1189–1205. doi:10.1175/1520-0485(1982)012<1189:DACOLS>2.0.CO;2
116. Trouet V, Esper J, Graham NE et al (2009) Persistent positive North Atlantic Oscillation mode dominated the medieval

climate anomaly. Science 324:78–80. doi:10.1126/science.1166349
117. Van Nieuwenhove N, Baumann A, Matthiessen J et al (2015) Sea surface conditions in the southern Nordic Seas during the Holocene based on dinoflagellate cyst assemblages. The Holocene
118. Vare LL, Massé G, Gregory TR et al (2009) Sea ice variations in the central Canadian Arctic Archipelago during the Holocene. Quat Sci Rev 28:1354–1366. doi:10.1016/j.quascirev.2009.01.013
119. Vellinga M, Wood RA (2002) Global climatic impacts of a collapse of the Atlantic thermohaline circulation. Clim Change 54:251–267. doi:10.1023/A:1016168827653
120. Wall D, Dale B (1966) "Living Fossils" in Western Atlantic Plankton. Nature 211:1025–1026. doi:10.1038/2111025a0
121. Weckström K, Massé G, Collins LG et al (2013) Evaluation of the sea ice proxy IP25 against observational and diatom proxy data in the SW Labrador Sea. Quat Sci Rev 79:53–62. doi:10.1016/j.quascirev.2013.02.012
122. Yao T (1986) The response of currents in Trinity Bay, Newfoundland, to local wind forcing. Atmos Ocean 24:235–252. doi:10.1080/07055900.1986.9649249
123. Yashayaev I (2007) Hydrographic changes in the Labrador Sea, 1960–2005. Prog Oceanogr 73:242–276. doi:10.1016/j.pocean.2007.04.015
124. Zabel M, Schneider RR, Wagner T et al (2001) Late quaternary climate changes in Central Africa as Inferred from Terrigenous Input to the Niger Fan. Quat Res 56:207–217. doi:10.1006/qres.2001.2261